Matrix Isolation Infrared Spectroscopic and Density Functional Theoretical Studies of the Reactions of Scandium Atoms with Methanol

Mohua Chen, Zhengguo Huang, and Mingfei Zhou*

Department of Chemistry & Laser Chemistry Institute, Shanghai Key Laboratory of Molecular Catalysts and Innovative Materials, Fudan University, Shanghai 200433, People's Republic of China

Received: April 15, 2004; In Final Form: May 17, 2004

The reactions of scandium atoms and methanol molecules have been investigated by matrix isolation infrared absorption spectroscopy. The reaction intermediates and products were identified on the basis of isotopic IR studies with $^{13}CH_3OH$, $CH_3{}^{18}OH$, and CH_3OD, as well as density functional theory calculations. In solid argon, the ground-state scandium atoms reacted with methanol to form the inserted CH_3OScH molecules spontaneously but not the thermodynamically more favorable CH_3ScOH. The inserted CH_3OScH molecule underwent photochemical rearrangement to form the $(CH_4)OSc$ complex upon ultraviolet−visible irradiation. In addition, the CH_3OSc molecule and its photoinduced CH_3ScO isomer were also observed.

Introduction

The catalytic conversion of methane to methanol has gained much attention due to its great economic and scientific importance.[1] The study of the $CH_4 + MO \rightarrow M + CH_3OH$ reaction and its reverse reaction can potentially provide quantitative information regarding the thermodynamics and mechanisms for the catalytic methane-to-methanol conversion process. Considerable studies have been focused on the gas-phase reactions of various transition metal oxide ions with methane.[2−4] The results showed that the late transition metal oxide ions can efficiently convert methane to methanol, while the early transition metal oxide ions cannot. In an $FeO^+ + CH_4$ reaction study, a $HOFe^+CH_3$ molecule has been suggested as a key intermediate in the reaction process.[2] Density functional calculations suggested that the $MO^+ + CH_4 \rightarrow M + CH_3OH$ reactions proceeded via the initial formation of a $OM^+(CH_4)$ complex followed by isomerization to the HOM^+CH_3 and $M^+(CH_3OH)$ intermediates via two transition states.[5] The results showed that the experimentally observed reaction efficiency and methanol-to-methyl branching ratio could be rationalized in terms of the predicted barrier heights at the transition states.

The reactions of neutral metal oxides with methane have received much less attention. Theoretical calculations showed that NiO and PdO are reactive toward methane and can form molecular complexes with CH_4 bound by 9−10 kcal/mol, but ScO is not reactive with respect to methane.[6] The insertion of these metal oxides into the C−H bond of methane leading to the CH_3MOH molecules (M = Sc, Ni, and Pd) was predicted to have significant energy barriers. No experimental studies have been reported on the reactions of neutral transition metal oxides with CH_4. However, the reactions of neutral metal atoms with methanol molecules have been studied by matrix isolation spectroscopy, a powerful method for delineating reaction mechanisms by facilitating the isolation and characterization of the reactive intermediates.[7−13] Previous studies have shown that metal atoms, in general, formed complexes with methanol molecules in solid matrixes. Photoexcitation of the complexes with visible or UV light induced oxidative insertion of the metal atoms into the O−H and/or C−O bonds of methanol. Recent investigations in our laboratory on the reactions of beryllium and magnesium atoms with methanol in solid argon have shown that the ground-state beryllium atoms spontaneously inserted into the O−H bond of methanol to form CH_3OBeH; the thermodynamically more favorable CH_3BeOH and CH_3MgOH were only formed upon broad-band irradiation.[12,13] In this paper, we report combined matrix isolation Fourier transform infrared (FTIR) spectroscopic and density functional theory (DFT) calculations on the reactions of Sc atoms with methanol.

Experimental and Theoretical Methods

The experimental setup for pulsed laser ablation and matrix isolation FTIR spectroscopic investigation has been described previously.[14] Briefly, the 1064 nm Nd:YAG laser fundamental (Spectra Physics, DCR 150, 20 Hz repetition rate and 8 ns pulse width) was focused onto the rotating scandium metal target, and the ablated metal atoms were codeposited with methanol in excess argon onto a 12 K CsI window for 1 h at a rate of approximately 2−4 mmol/h. Typically, 5−10 mJ/pulse laser power was used. Methanol was subjected to several freeze−pump−thaw cycles to minimize possible atmospheric contamination. The isotopic CH_3OD (Merck, 99%) and $^{13}CH_3OH$ and $CH_3{}^{18}OH$ (99%, Cambridge Isotopic Laboratories) and selected mixtures were used in different experiments. Infrared spectra were recorded on a Bruker IFS 113V spectrometer at 0.5 cm^{-1} resolution by use of a DTGS detector. Matrix samples were annealed at different temperatures, and selected samples were subjected to broad-band irradiation with a 250 W high-pressure mercury arc lamp.

Density functional calculations were performed with the Gaussian 98 program.[15] The three-parameter hybrid functional according to Becke with additional correlation corrections due to Lee, Yang, and Parr (B3LYP) and the 6-311++G** basis sets were utilized.[16−19] The geometries were fully optimized; the harmonic vibrational frequencies were calculated with analytic second derivatives, and zero-point vibrational energies (ZPVE) were derived. Transition-state optimizations were done with the synchronous transit-guided quasi-Newton (STQN) method[20] at the B3LYP/6-311++G** level followed by the

* Corresponding author: e-mail mfzhou@fudan.edu.cn.

10.1021/jp048348u CCC: $27.50
Published on Web 06/22/2004

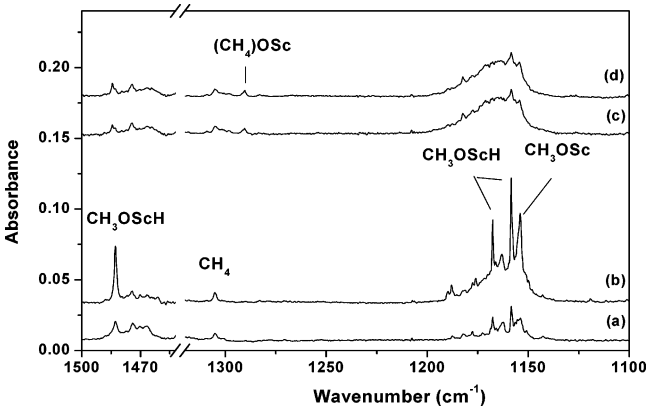

Figure 1. Infrared spectra in the 1500−1450 and 1320−1100 cm^{-1} regions from codeposition of laser-ablated scandium atoms with 0.2% CH_3OH in argon: (a) 1 h of sample deposition at 12 K, (b) after 24 K annealing, (c) after 30 min of broad-band irradiation, and (d) after 30 K annealing.

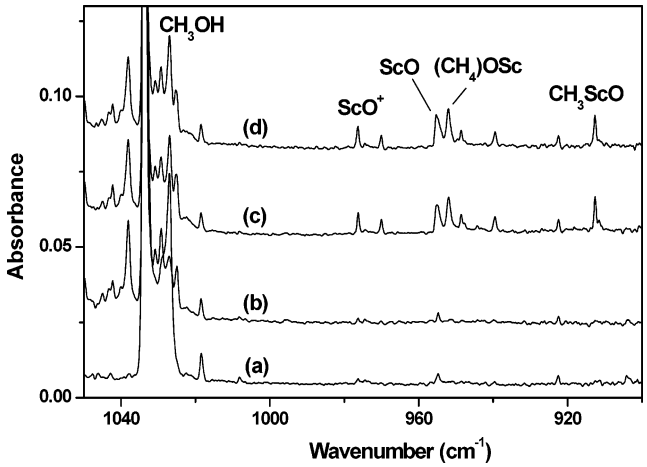

Figure 2. Infrared spectra in the 1050−900 cm^{-1} region from codeposition of laser-ablated scandium atoms with 0.2% CH_3OH in argon: (a) 1 h of sample deposition at 12 K, (b) after 24 K annealing, (c) after 30 min of broad-band irradiation, and (d) after 30 K annealing.

vibrational frequency calculations showing the obtained structures to be true saddle points.

Results and Discussion

The infrared spectra of the reaction products were reported, and the product absorptions will be assigned by consideration of the frequencies, isotopic shifts, and splittings of the observed bands and by comparisons with theoretical frequency calculations.

Infrared Spectra. The infrared spectra in selected regions from co-condensation of laser-ablated Sc atoms with 0.2% methanol in argon are shown in Figures 1 and 2, respectively, and the product absorptions are listed in Table 1. The behaviors of the product absorptions upon stepwise annealing and broad-band irradiation are also shown in the figures. After sample deposition, very strong CH_3OH absorptions and weak CH_4 absorption (1305.4 cm^{-1})[21] were observed. Weak absorptions due to CH_2OH (1182.7 and 1047.5 cm^{-1}),[22] H_2CO (1742.1 cm^{-1}), and HCO (1863.4 and 1084.8 cm^{-1})[23] formed from CH_3OH fragmentation were also observed when relatively high laser energy was employed. Besides the above-mentioned absorptions, new product absorptions at 1482.7, 1167.4, 1158.5, and 1154.3 (Figures 1 and 2, trace a) and at 583.5 and 562.2 cm^{-1} (not shown) were observed after sample deposition. These product absorptions markedly increased on sample annealing to 24 K (Figures 1 and 2, trace b). Subsequent broad-band irradiation with the high-pressure mercury arc lamp destroyed these absorptions, and produced new absorptions at 1290.5, 952.1, and 912.7 cm^{-1}, as well as the ScO^+ (976.4 cm^{-1}) and ScO (954.9 cm^{-1}) absorptions.[24] The ScO^+ and ScO absorptions and the 1290.5, 952.1, and 912.7 cm^{-1} absorptions remained almost unchanged upon further annealing to 30 K (Figures 1 and 2, trace d).

TABLE 1: Infrared Absorptions[a] from Codeposition of Laser-Ablated Scandium Atoms with Methanol in Excess Argon

$CH_3{}^{16}OH$	$CH_3{}^{18}OH$	$^{13}CH_3OH$	CH_3OD	assignment
1482.7	1482.7	1482.7	1063.5	CH_3OScH, ν(Sc−H)
1290.5	1290.5	1283.0		$(CH_4)OSc$, $\delta(CH_2)$
1167.4				CH_3OScH, $\delta(CH_3)$
1158.5	1126.3	1142.9	1160.1	CH_3OScH, ν(C−O)
1154.3	1118.7	1137.6	1154.3	CH_3OSc, ν(C−O)
952.1	912.3	952.1	952.1	$(CH_4)OSc$, ν(Sc−O)
912.7	874.8	912.6	912.7	CH_3ScO, ν(Sc−O)
583.5	578.7	574.5	583.5	CH_3OSc, ν(Sc−O)
562.2	556.4	554.7		CH_3OScH, ν(Sc−O)

[a] IR absorption values are given in reciprocal centimeters.

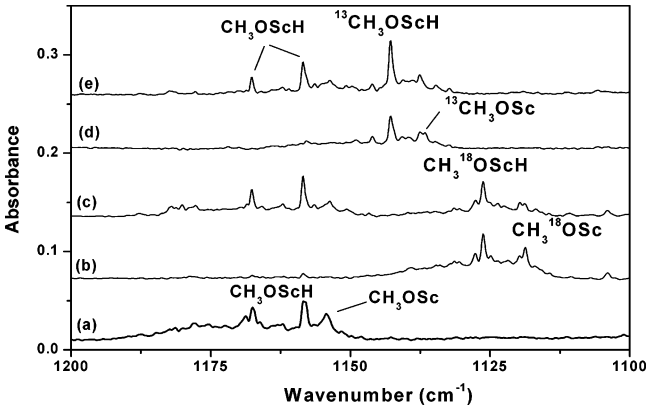

Figure 3. Infrared spectra in the 1200−1100 cm^{-1} region from codeposition of laser-ablated scandium atoms with isotopic substituted CH_3OH in excess argon. Spectra were taken after 1 h of sample deposition followed by 24 K annealing: (a) 0.2% CH_3OH, (b) 0.2% $CH_3{}^{18}OH$, (c) 0.1% $CH_3{}^{16}OH$ + 0.1% $CH_3{}^{18}OH$, (d) 0.2% $^{13}CH_3OH$, and (e) 0.1% $^{12}CH_3OH$ + 0.1% $^{13}CH_3OH$.

Experiments were repeated with the $^{13}CH_3OH$, $CH_3{}^{18}OH$, $^{12}CH_3OH$ + $^{13}CH_3OH$, $CH_3{}^{16}OH$ + $CH_3{}^{18}OH$, and CH_3OH + CH_3OD samples. The isotopic frequencies are also listed in Table 1. The infrared spectra in selected regions for different isotopic samples are shown in Figures 3−5.

Calculation Results. DFT/B3LYP calculations were performed on the potential reaction products. Five $ScCH_3OH$ structural isomers, namely, the $Sc(CH_3OH)$ and $(CH_4)OSc$ complexes and the inserted CH_3ScOH, CH_3OscH, and $HScCH_2OH$ molecules were considered. The optimized geometric parameters are shown in Figure 6, and the vibrational frequencies and intensities are listed in Table 2. All five structural isomers were predicted to be local minima on the doublet potential energy surface and to be stable with respect to the ground-state reactants: Sc + CH_3OH.

Similar calculations were also done on the CH_3OSc and CH_3ScO molecules. The optimized structures are also shown in Figure 6, and the vibrational frequencies and intensities are listed in Table 2.

CH_3OScH. Absorptions at 1482.7, 1167.4, 1158.5, and 562.2 cm^{-1} are assigned to the CH_3OScH molecule. These bands

TABLE 2: Calculated Vibrational Frequencies and Intensities of the $ScCH_3OH$ and CH_3ScO Isomers at the B3LYP/6-311++G Level**

molecule	frequency (intensity)
$Sc(CH_3OH)$ ($^2A''$)	3645.1 (309), 3159.7 (6), 3129.8 (8), 3050.7 (38), 1498.0 (14), 1491.7 (1), 1454.6 (13), 1332.8 (91), 1156.0 (2), 1070.1 (53), 966.8 (53), 292.0 (9), 263.1 (12), 139.2 6), 60.2 (1)
CH_3OScH ($^2A'$)	3052.9 (33), 3052.1(39), 2991.4 (131), 1522.2 (485), 1494.1 (3), 1493.3 (5), 1473.4 (17), 1172.8 (245), 1169.3 (2), 1163.7 (276), 553.4 (86), 314.6 (68), 171.1 (46), 141.4 (14), 29.5 (35)
CH_3ScOH ($^2A'$)	3962.1 (218), 3052.1 (8), 3036.8 (13), 2968.0 (11), 1430.0 (14), 1423.3 (0), 1149.1 (22), 707.7 (182), 495.6 (67), 416.8 (17), 396.4 (40), 357.2 (83), 338.0 (145), 119.3 (2), 18.9 (0)
$(CH_4)OSc$ ($^2A_1$)	3130.2 (0), 3115.2 (32 × 2), 3013.7 (17), 1565.2 (0 × 2), 1354.5 (12 × 2), 1329.5 (14), 996.6 (250), 147.8 (1 × 2), 55.9 (1), 44.9 (16 × 2)
CH_3OSc ($^1A_1$)	3076.9 (21 × 2), 3007.3 (107), 1490.3 (5 × 2), 1470.7 (4), 1185.1 (425), 1164.7 (1 × 2), 584.6 (15), 161.5 (7 × 2)
CH_3ScO ($^1A'$)	3048.0 (22), 3046.1 (30), 2977.5 (33), 1442.5 (1), 1435.3 (1), 1140.3 (2), 965.3 (289), 517.4 (32), 453.5 (70), 423.7 (70), 151.8 (19), 53.5 (13)

[a] Vibrational frequencies are given in reciprocal centimeters; intensities (in parentheses) are given in kilometers per mole.

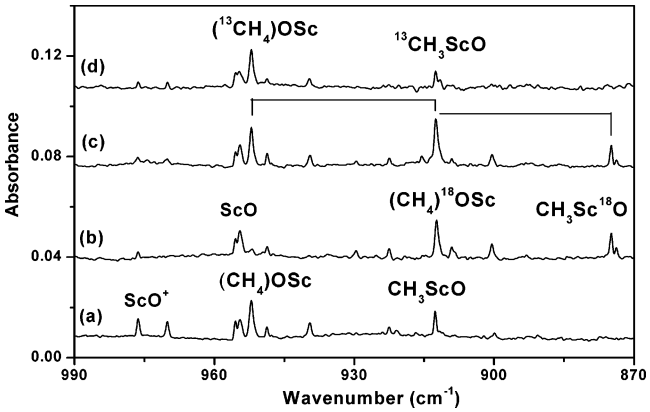

Figure 4. Infrared spectra in the 990−870 cm^{-1} region from codeposition of laser-ablated scandium atoms with isotopic substituted CH_3OH in excess argon. Spectra were taken after 1 h of sample deposition followed by 24 K annealing and 30 min broad-band irradiation: (a) 0.2% CH_3OH, (b) 0.2% $CH_3{}^{18}OH$, (c) 0.1% $CH_3{}^{16}OH$ + 0.1% $CH_3{}^{18}OH$, and (d) 0.2% $^{13}CH_3OH$.

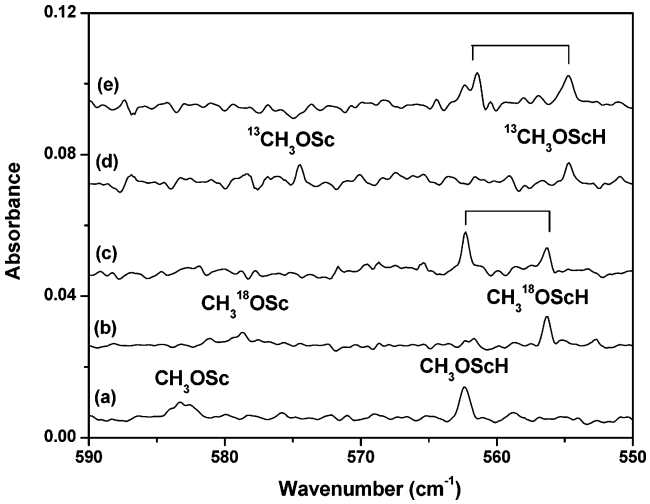

Figure 5. Infrared spectra in the 590−550 cm^{-1} region from codeposition of laser-ablated scandium atoms with isotopic substituted CH_3OH in excess argon. Spectra were taken after 1 h of sample deposition followed by 24 K annealing: (a) 0.2% CH_3OH, (b) 0.2% $CH_3{}^{18}OH$, (c) 0.1% $CH_3{}^{16}OH$ + 0.1% $CH_3{}^{18}OH$, (d) 0.2% $^{13}CH_3OH$, and (e) 0.1% $^{12}CH_3OH$ + 0.1% $^{13}CH_3OH$.

exhibited the same relative intensities in experiments with different laser energy and CH_3OH concentrations, suggesting that these bands are due to different vibrational modes of the same molecule. The 1482.7 cm^{-1} band showed no isotopic frequency shift when $CH_3{}^{18}OH$ and $^{13}CH_3OH$ samples were used. It shifted to 1063.5 cm^{-1} with CH_3OD. The H/D isotopic frequency ratio of 1.3942 is indicative of a Sc−H stretching vibration. Both the band position and isotopic frequency ratio

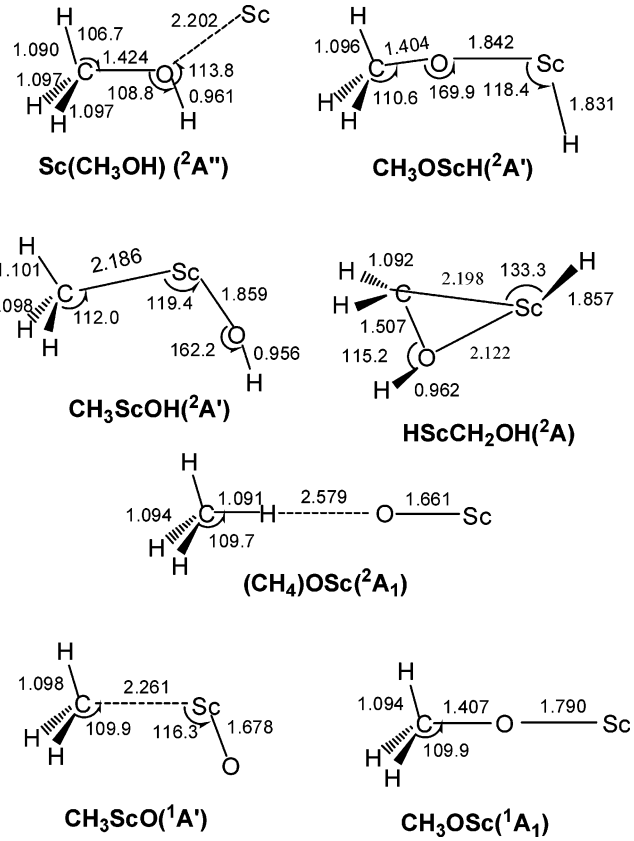

Figure 6. Optimized structures (bond lengths in angstroms, bond angles in degrees) of the $ScCH_3OH$ and CH_3ScO isomers.

are very close to those of the Sc−H stretching mode of HScOH in solid argon (1482.6 cm^{-1} with H/D ratio of 1.3876).[25] The 1158.5 cm^{-1} band is assigned to the C−O stretching mode. This band shifted to 1126.3 cm^{-1} with $CH_3{}^{18}OH$ and to 1142.9 cm^{-1} with $^{13}CH_3OH$, giving $^{16}O/^{18}O$ and $^{12}C/^{13}C$ isotopic frequency ratios of 1.0286 and 1.0136, respectively. In the mixed $CH_3{}^{16}OH$ + $CH_3{}^{18}OH$ (Figure 3, trace c) and $^{12}CH_3OH$ + $^{13}CH_3OH$ (Figure 3, trace e) experiments, only the pure isotopic counterparts were observed, indicating that only one CO subunit is involved in the molecule. The 1167.4 cm^{-1} band is assigned to the CH_3 deformation mode. The carbon-13 and oxygen-18 counterparts of the 1167.4 cm^{-1} band could not be observed due to isotopic effect. The 562.2 cm^{-1} band is due to Sc−O stretching vibration. This band shifted to 556.4 cm^{-1} with $CH_3{}^{18}OH$ and to 554.7 cm^{-1} with $^{13}CH_3OH$. In the mixed $CH_3{}^{16}OH$ + $CH_3{}^{18}OH$ (Figure 5, trace c) and $^{12}CH_3OH$ + $^{13}CH_3OH$ (Figure 5, trace e) experiments, only the pure isotopic counterparts were observed.

The assignment is supported by the DFT calculations. As shown in Figure 6, CH_3OScH was predicted to have a $^2A'$

TABLE 3: Comparison of the Observed and Calculated Vibrational Frequencies[a] and Isotopic Frequency Ratios of the Observed Products

		freq		$^{16}O/^{18}O$		$^{12}C/^{13}C$	
molecule	mode	obs	calc	obs	calc	obs	calc
CH_3OScH	ν(Sc−H)	1482.7	1522.2	1.0000	1.0000	1.0000	1.0000
	$\delta(CH_3)$	1167.4	1172.8		1.0057		1.0091
	ν(C−O)	1158.5	1163.7	1.0286	1.0317	1.0136	1.0131
	ν(Sc−O)	562.2	553.4	1.0104	1.0097	1.0135	1.0139
CH_3OSc	ν(C−O)	1154.3	1185.1	1.0318	1.0367	1.0147	1.0139
	ν(Sc−O)	583.5	584.6	1.0083	1.0079	1.0157	1.0162
$(CH_4)OSc$	$\delta(CH_2)$	1290.5	1354.5	1.0001	1.0000	1.0058	1.0062
	ν(Sc−O)	952.1	996.6	1.0436	1.0438	1.0000	1.0000
CH_3ScO	ν(Sc−O)	912.7	965.3	1.0433	1.0436	1.0001	1.0001

[a] Vibrational frequencies are given in reciprocal centimeters.

ground state with C_s symmetry. The Sc−H stretching, CH_3 deformation, C−O stretching, and Sc−O stretching modes were computed at 1522.2, 1172.8, 1163.7, and 553.4 cm^{-1} with 485, 245, 276, and 86 km/mol IR intensities, respectively, which are in excellent agreement with the experimental values. The C−H stretching modes were also predicted to have appreciable IR intensities but may be overlapped by the strong CH_3OH absorptions. As listed in Table 3, the calculated isotopic frequency ratios for the three stretching modes fit the experimental values very well. Moreover, the calculated relative intensities of the CH_3 deformation and C−O stretching modes for different CH_3OScH isotopomers are in complete accord with the experimental observations. Experimentally, both the CH_3 deformation and C−O stretching modes were observed in the CH_3OH experiments, but only one mode was observed in the $^{13}CH_3OH$ and $CH_3{}^{18}OH$ experiments. As listed in Table 2, the predicted IR intensity of the CH_3 deformation mode (245 km/mol) is comparable to that of the C−O stretching mode (276 km/mol). The frequencies of these two modes were predicted at 1166.1 and 1127.9 cm^{-1} with 8 and 459 km/mol IR intensities for the $CH_3{}^{18}OScH$ isotopomer and at 1162.2 and 1148.7 cm^{-1} with 75 and 447 km/mol IR intensities for the $^{13}CH_3OScH$ isotopomer. This suggests that there is coupling between the CH_3 deformation mode and the C−O stretching mode. The frequencies of these two modes of CH_3OScH are very close. The CH_3 deformation mode may gain intensity via strong coupling with the C−O stretching mode. The coupling effect became weaker in the $CH_3{}^{18}OScH$ and $^{13}CH_3OScH$ isotopomers, as the frequency differences between two vibrational modes are larger than that in CH_3OScH.

$(CH_4)OSc$. The 1290.5 and 952.1 cm^{-1} absorptions appeared together on broad-band irradiation. The 952.1 cm^{-1} band is only 2.8 cm^{-1} lower than the Sc−O stretching frequency of ScO in solid argon. This band exhibited no shift with $^{13}CH_3OH$ and CH_3OD but shifted to 912.3 cm^{-1} in the $CH_3{}^{18}OH$ experiment. The $^{16}O/^{18}O$ isotopic frequency ratio of 1.0436 is about the same as the ratio of diatomic ScO (1.0434). The mixed $CH_3{}^{16}OH$ + $CH_3{}^{18}OH$ spectrum (Figure 4, trace c) clearly indicates that only one O atom is involved in this mode. These observations indicate that the 952.1 cm^{-1} band is due to a terminal Sc−O stretching vibration of a ScO complex. The 1290.6 cm^{-1} band showed no shift with $CH_3{}^{18}OH$ but shifted to 1283.0 cm^{-1} when the $^{13}CH_3OH$ sample was used. The band position and isotopic frequency shift suggest the assignment of this band to a CH_2 deformation mode. The triply degenerated CH_2 deformation mode of CH_4 was observed at 1305.4 cm^{-1}. Accordingly, we assign the 1290.5 and 952.1 cm^{-1} bands to the $(CH_4)OSc$ complex.

The $(CH_4)OSc$ complex was predicted to have a $^2A_1$ ground state with C_{3v} symmetry. The complex was predicted to be coordinated between the O atom of the ScO subunit and one of the H atoms of the CH_4 subunit. The small deformation of the CH_4 and ScO subunits and the rather long O−H distance (2.579 Å) indicate weak interaction between the CH_4 and ScO subunits. The binding energy with respect to ScO + CH_4 was predicted to be only 0.4 kJ/mol, significantly lower than that of the (CH_4)-NiO and (CH_4)PdO complexes, which were predicted to be coordinated between the metal and C atoms.[6] The Sc−O stretching frequency was predicted to red-shift about 3.2 cm^{-1} by CH_4 complexation, consistent with the observed shift of 2.8 cm^{-1}. However, the calculation predicted the CH_2 deformation mode to be blue-shifted from that of CH_4, in disagreement with the experimental observation. It is known that B3LYP is not good at predicting some loosely bound weak complexes.

CH_3OSc. The 1154.3 and 583.5 cm^{-1} bands appeared together on annealing. The upper band shifted to 1118.7 cm^{-1} with $CH_3{}^{18}OH$ and to 1137.6 cm^{-1} with $^{13}CH_3OH$. The $^{16}O/^{18}O$ and $^{12}C/^{13}C$ isotopic frequency ratios of 1.0318 and 1.0147 are very similar to those of the C−O stretching vibration of the above-characterized CH_3OScH molecule, which suggests that the 1154.3 cm^{-1} band is due to a C−O stretching vibration. In concert, the lower band went to 578.7 cm^{-1} in the $CH_3{}^{18}OH$ experiment and to 574.5 cm^{-1} when the $^{13}CH_3OH$ sample was used; the $^{16}O/^{18}O$ isotopic frequency ratio of 1.0083 and the $^{12}C/^{13}C$ isotopic frequency ratio of 1.0157 are quite similar to those of the Sc−O stretching mode of CH_3OScH. These observations imply the involvement of a CH_3OSc unit in the new species. No absorptions in the Sc−H stretching frequency regions were observed to track the 1154.3 and 583.5 cm^{-1} bands. Therefore, we assign the 1154.3 and 583.5 cm^{-1} bands to the C−O and Sc−O stretching vibrations of CH_3OSc. The C−O stretching frequency of CH_3OSc red-shifted by 4.2 cm^{-1}, whereas the Sc−O stretching frequency blue-shifted by 21.2 cm^{-1}, when compared to the frequencies of the corresponding vibrations in CH_3OScH. As shown in Figure 6, the CH_3OSc molecule was predicted to have a $^1A_1$ ground state with C_{3v} symmetry. As listed in Tables 2 and 3, the calculated C−O and Sc−O stretching frequencies and isotopic frequency ratios matched the experimental values very well. The geometry parameters of CH_3OSc are very similar to those of the CH_3-OSc subunit in CH_3OScH, with the C−O bond length 0.003 Å longer and the Sc−O bond length 0.052 Å shorter. These bond differences are consistent with the relative frequency shifts of the C−O and Sc−O stretching modes mentioned above.

CH_3ScO. The band at 912.7 cm^{-1} appeared on broad-band irradiation. This band showed a very small C-13 shift (0.1 cm^{-1}) but a large O-18 shift (to 874.8 cm^{-1} in the $CH_3{}^{18}OH$ experiment). The $^{16}O/^{18}O$ isotopic frequency ratio of 1.0433 is about the same as the diatomic ScO ratio (1.0434). In the mixed $CH_3{}^{16}OH$ + $CH_3{}^{18}OH$ spectrum (Figure 4, trace c), only the pure isotopic counterparts were observed, indicating that only one O atom is involved in the mode. The small shift with $^{13}CH_3$-OH suggests that this mode is very weakly coupled to another structural subunit involving C. The 912.7 cm^{-1} band is assigned to the Sc−O stretching mode of CH_3ScO. In the Sc + H_2O reaction, the HScO molecule was produced on broad-band irradiation and has a Sc−O stretching mode at 922.3 cm^{-1}.[25] DFT calculations predicted the CH_3ScO molecule to have a $^1A'$ ground state with C_s symmetry. The Sc−O stretching mode of CH_3ScO was predicted at 965.3 cm^{-1}. This mode has the largest IR intensity. The Sc−O stretching frequency of HScO was calculated to be 977.4 cm^{-1} at the same level of theory.[25] The frequency difference between HScO and CH_3ScO, 12.1 cm^{-1},

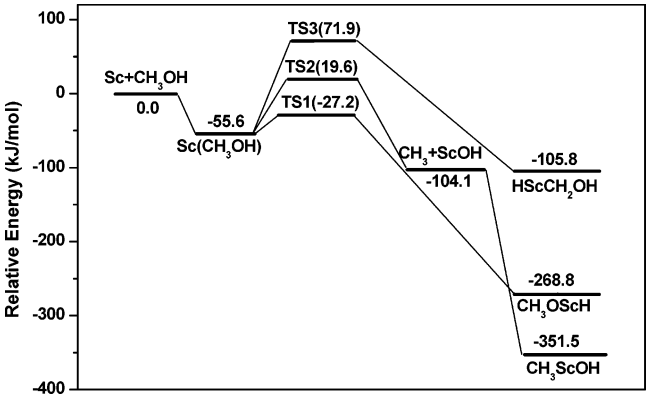

Figure 7. Potential energy profile for the reaction of Sc + CH_3OH (relative energies are given in kilojoules per mole).

is in good agreement with the experimentally observed frequency difference of 9.6 cm^{-1}.

Reaction Mechanisms. Previous matrix isolation studies on the reactions of metal atoms with methanol in solid matrixes have shown that the primary reaction, in general, is the formation of the 1:1 metal−methanol complex.[7−13] The Sc(CH_3OH) complex was predicted to have a $^2A''$ ground state with C_s symmetry. The Sc(CH_3OH) complex has been calculated by Hwang and Mebel[6] at the B3LYP/6-31G(d,p) and B3LYP/6-311+G(3df,2p) levels.[6] The Sc(CH_3OH) complex was predicted to have C_1 symmetry. We note that the present calculated C_s geometry is actually very similar to that of Hwang and Mebel's C_1 geometry, the only difference being the relative positions of the H atoms in the CH_3 subunit. The complex was predicted to have quite strong O−H and C−O stretching vibrations (Table 2), which were red-shifted from those of free CH_3OH. In our experiment, no evidence was found for the formation of the Sc(CH_3OH) complex. On the contrary, the CH_3OScH absorptions markedly increased on annealing. The CH_3OScH molecules were formed by the ground-state Sc atom insertion into the O−H bond of methanol, reaction 1, which was predicted to be exothermic and requires no activation energy:

$$Sc\ (^2D) + CH_3OH \rightarrow CH_3OScH\ (^2A') \qquad (1)$$

Previous studies on the reactions of metal atoms and methanol showed that the metal atoms could insert into not only the O−H bond but also the C−O bond of methanol.[7−13] The C−O bond insertion product CH_3ScOH was predicted to have a $^2A'$ ground state with C_s symmetry (Figure 6), in agreement with the previous theoretical calculations.[6] The CH_3ScOH molecule was predicted to be 82.8 kJ/mol more stable than the CH_3OScH isomer. It is very interesting to note that ground-state Sc atoms reacted with methanol to form CH_3OScH but not the thermodynamically more favorable CH_3ScOH. To have a better understanding of the experimental observations, potential energy profiles on the doublet surfaces of the Sc(^2D) + CH_3OH reaction were calculated at the B3LYP/6-311++G(d,p) level. The results are shown in Figures 7 and 8. Similar to the previously reported metal atom and methanol reactions, the initial step of the Sc + CH_3OH reaction is the formation of the Sc(CH_3OH) complex,[12,13] which proceeds without any energy barrier. DFT calculations showed that this reaction was exothermic by about 55.6 kJ/mol. From the complex, three reaction paths are possible. The first path is the Sc atom insertion into the O−H bond of methanol to form CH_3OScH via a transition state (TS1). The second path is the formation of the ScOH + CH_3 dissociation products via a transition state (TS2); the CH_3 + ScOH products

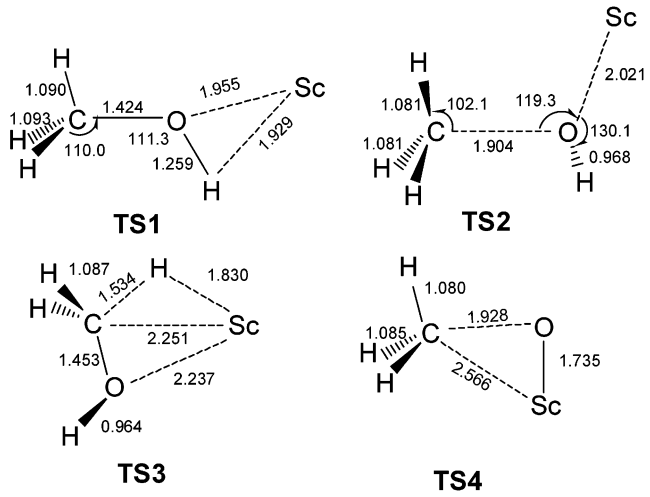

Figure 8. Optimized structures (bond lengths in angstroms, bond angles in degrees) of the transition states on the potential energy profiles shown in Figure 7.

can recombine to form the CH_3ScOH molecule without energy barrier, as the previous theoretical study indicated.[6] The third path is the Sc atom insertion into the C−H bond of methanol to form $HScCH_2OH$ via a transition state (TS3). The $HScCH_2OH$ molecule was predicted to have a three-membered ring structure with Sc−C and Sc−O bond lengths of 2.198 and 2.123 Å. The transition state (TS3) exhibited longer Sc−C and Sc−O bond lengths and shorter Sc−H bond length than those of $HScCH_2OH$. The intrinsic reaction coordination (IRC) calculations confirmed the energy paths from the transition structures to the corresponding minima. All three insertion products were stable with respect to the Sc(CH_3OH) complex. The $HScCH_2OH$ molecule is less stable than the other two insertion molecules, and the C−H bond insertion path proceeds via the highest energy barrier. Although the CH_3OScH molecule lies higher in energy than the CH_3ScOH isomer, the energy barrier for the formation of CH_3OScH is 46.8 kJ/mol lower than the energy barrier for the formation of CH_3ScOH. Moreover, both the transition states for the formation of $HScCH_2OH$ and CH_3ScOH lie higher in energy than the ground-state reactants, Sc (^2D) + CH_3OH ($^1A'$), whereas the transition state for the formation of CH_3OScH lies 19.6 kJ/mol lower in energy than the ground-state reactants. As the formation of the Sc(CH_3OH) complex is initially exothermic by 55.6 kJ/mol, which is sufficient to surmount the energy barrier for the O−H bond insertion reaction, the formation of CH_3OScH is spontaneous in solid argon. This also suggests that the Sc(CH_3OH) complex is very short-lived, rapidly rearranging to form the CH_3OScH molecule.

The CH_3OScH absorptions were destroyed under broad-band UV−visible light irradiation, during which the $(CH_4)OSc$ complex absorptions increased. It appears that UV−visible light initiates isomerization reaction 2:

$$CH_3OScH + h\nu \rightarrow (CH_4)OSc \qquad (2)$$

DFT calculations predicted that the $(CH_4)OSc$ complex is 41.0 kJ/mol more stable than the CH_3OScH isomer. This process requires activation energy. We tried to calculate the energy barrier for this process but failed to locate a transition state, which suggests that the process may not be a one-step reaction. A recent theoretical study on the CH_3ScOH to ScO + CH_4 reaction found a transition state lying 134.6 kJ/mol higher in energy than CH_3ScOH.

Besides the above-mentioned product molecules, the CH_3OSc absorptions were also observed to increase on annealing. CH_3OSc could be formed either by preliminary Sc insertion into the O−H bond via a CH_3OScH intermediate, followed by H atom detachment, or by CH_3O + Sc association reaction in solid argon. The formation from Sc + CH_3OH was predicted to be endothermic by about 2 kJ/mol and hence does not seem very likely. The CH_3O + Sc reaction is exothermic. Condensation of laser-ablated Sc atoms with CH_3OH in excess argon at 12 K resulted in partial fragmentation of CH_3OH. Weak absorptions due to CH_2OH, H_2CO, and HCO were observed when relatively high laser energy was employed. Although the infrared absorption spectrum of CH_3O in solid argon has not been reported, it has been trapped in solid argon and detected by laser-induced fluorescence spectroscopy.[26]

The CH_3OSc absorptions disappeared on broad-band irradiation, during which the CH_3ScO absorption was produced. This suggests that CH_3ScO was formed by photoinduced isomerization of CH_3OSc, reaction 3:

$$CH_3OSc + h\nu \rightarrow CH_3ScO \qquad (3)$$

The CH_3ScO molecule was predicted to be 92.4 kJ/mol more stable than the CH_3OSc isomer. This isomerization reaction was predicted to proceed via a transition state (TS4, as shown in Figure 8) with an energy barrier of 143.8 kJ/mol.

From the results on the reactions of Mg, Be, and Sc atoms with CH_3OH, some trends can be observed. For all three metal atoms, the O−H bond insertion CH_3OMH (M = Mg, Be, and Sc) products are thermodynamically less stable than the C−O bond insertion CH_3MOH products. However, the energy barrier for the O−H bond insertion process is lower than that for the C−O bond insertion process. The CH_3OMH molecules are potential important intermediates on the potential energy surfaces of the M + $CH_3OH \leftrightarrow$ MO + CH_4 reactions, which have not been considered in most previous studies.[2−6]

Conclusions

The reactions of Sc atoms with methanol molecules have been investigated with matrix isolation FTIR spectroscopy and theoretical calculations. In solid argon, ground-state Sc atoms directly inserted into the O−H bond of methanol to form the CH_3OScH molecule without activation energy. The CH_3OScH molecule underwent photochemical rearrangement to form the $(CH_4)OSc$ complex upon broad-band UV−visible irradiation. Theoretical analysis showed that the CH_3OScH molecule is less stable than the C−O bond insertion product CH_3ScOH. However, the energy barrier for the O−H bond insertion process was predicted to be lower than that of the C−O bond insertion process, and the transition state lies lower in energy than the ground-state reactants, consistent with the experimental observations. In addition, the CH_3OSc molecule, which may be formed by the CH_3O + Sc reaction, was also observed. UV−Visible irradiation resulted in the isomerization of CH_3OSc to the more stable CH_3ScO isomer.

Acknowledgment. We gratefully acknowledge financial support from NSFC (20125311) and the NKBRSF of China.

References and Notes

(1) Gesser, H. D.; Hunter, N. R.; Prakash, C. B. *Chem. Rev.* **1988**, *85*, 235.
(2) Schröder, D.; Schwarz, H. *Angew. Chem., Int. Ed. Engl.* **1990**, *29*, 1433.
(3) (a) Schroder, D.; Fiedler, A.; Hrusak, J.; Schwarz, H. *J. Am. Chem. Soc*. **1992**, *114*, 1215. (b) Ryan, M. F.; Fiedler, A.; Schroder, D.; Schwarz, H. *J. Am. Chem. Soc*. **1995**, *117*, 2033. (c) Ryan, M. F.; Fiedler, A.; Schroder, D.; Schwarz, H. *Organometallics* **1994**, *13*, 4072. (d) Schroder, D.; Schwarz, H. *Angew. Chem., Int. Ed. Engl.* **1995**, *34*, 1973.
(4) (a) Clemmer, D. E.; Aristov, N.; Armentrout, P. B. *J. Phys. Chem*. **1993**, *97*, 544. (b) Chen, Y. M.; Clemmer, D. E.; Armentrout, P. B. *J. Am. Chem. Soc*. **1994**, *116*, 7815.
(5) (a) Yoshizawa, K.; Shiota, Y.; Yamabe, T. *Chem. Eur. J.* **1997**, *3*, 1160. (b) Yoshizawa, K.; Shiota, Y.; Yamabe, T. *J. Am. Chem. Soc*. **1998**, *120*, 564. (c) Shiota, Y.; Yoshizawa, K. *J. Am. Chem. Soc.* **2000**, *122*, 12317.
(6) Hwang, D. Y.; Mebel, A. M. *J. Phys. Chem. A* **2002**, *106*, 12072.
(7) Park, M.; Hauge, R. H.; Kafafi, Z. H.; Margrave, J. L. *J. Chem. Soc., Chem. Commun.* **1985**, 1570.
(8) Maier, G.; Reisenauer, H. P.; Egenolf, H. *Monatsh. Chem.* **1999**, *130*, 227.
(9) Khabashesku, V. N.; Kudin, K. N.; Margrave, J. L.; Fredin, L. *J. Organomet. Chem*. **2000**, *595*, 248.
(10) Lanzisera, D. V.; Andrews, L. *J. Phys. Chem. A* **1997**, *101*, 1482.
(11) Joly, H. A.; Howard, J. A.; Arteca, G. A. *Phys. Chem. Chem. Phys.* **2001**, *3*, 750.
(12) Huang, Z. G.; Chen, M. H.; Liu, Q. N.; Zhou, M. F. *J. Phys. Chem. A* **2003**, *107*, 11380.
(13) Huang, Z. G.; Chen, M. H.; Zhou, M. F. *J. Phys. Chem. A* **2004**, *108*, 3390.
(14) Chen, M. H.; Wang, X. F.; Zhang, L. N.; Yu, M.; Qin, Q. Z. *Chem. Phys*. **1999**, *242*, 81.
(15) Frisch, M. J.; Trucks, G. W.; Schlegel, H. B.; Scuseria, G. E.; Robb, M. A.; Cheeseman, J. R.; Zakrzewski, V. G.; Montgomery, J. A., Jr.; Stratmann, R. E.; Burant, J. C.; Dapprich, S.; Millam, J. M.; Daniels, A. D.; Kudin, K. N.; Strain, M. C.; Farkas, O.; Tomasi, J.; Barone, V.; Cossi, M.; Cammi, R.; Mennucci, B.; Pomelli, C.; Adamo, C.; Clifford, S.; Ochterski, J.; Petersson, G. A.; Ayala, P. Y.; Cui, Q.; Morokuma, K.; Malick, D. K.; Rabuck, A. D.; Raghavachari, K.; Foresman, J. B.; Cioslowski, J.; Ortiz, J. V.; Baboul, A. G.; Stefanov, B. B.; Liu, G.; Liashenko, A.; Piskorz, P.; Komaromi, I.; Gomperts, R.; Martin, R. L.; Fox, D. J.; Keith, T.; Al-Laham, M. A.; Peng, C. Y.; Nanayakkara, A.; Gonzalez, C.; Challacombe, M.; Gill, P. M. W.; Johnson, B.; Chen, W.; Wong, M. W.; Andres, J. L.; Gonzalez, C.; Head-Gordon, M.; Replogle, E. S.; Pople, J. A. Gaussian 98, Revision A.7; Gaussian, Inc.: Pittsburgh, PA, 1998.
(16) Becke, A. D. *J. Chem. Phys*. **1993**, *98*, 5648.
(17) Lee, C.; Yang, E.; Parr, R. G. *Phys. Rev. B* **1988**, *37*, 785.
(18) McLean, A. D.; Chandler, G. S. *J. Chem. Phys*. **1980**, *72*, 5639.
(19) Krishnan, R.; Binkley, J. S.; Seeger, R.; Pople, J. A. *J. Chem. Phys*. **1980**, *72*, 650.
(20) Head-Gordon, M.; Pople, J. A.; Frisch, M. *Chem. Phys. Lett*.**1988**, *153*, 503.
(21) Ogawara, Y.; Bruneau, A.; Kimura, T. *Anal. Chem.* **1994**, *66*, 4354.
(22) (a) Jacox, M. E.; Milligan, D. E. *J. Mol. Spectrosc*. **1973**, *47*, 148. (b) Jacox, M. E. *Chem. Phys.* **1981**, *59*, 213.
(23) Milligan, D. E.; Jacox, M. E. *J. Chem. Phys*. **1969**, *51*, 277.
(24) Bauschlicher, C. W., Jr.; Zhou, M. F.; Andrews, L.; Johnson, J. R. T.; Panas, I.; Snis, A. *J. Phys. Chem. A* **1999**, *103*, 5463 and references therein.
(25) Zhang, L. N.; Dong, J.; Zhou, M. F. *J. Phys. Chem. A* **2000**, *104*, 8882.
(26) Chiang, S. Y.; Hsu, Y. C.; Lee, Y. P. *J. Chem. Phys*. **1989**, *90*, 81.